MEAN-FIELD APPROACH TO COMPRESSION OF THICK POROUS FIBRE NETWORKS

J. A. Ketoja[1], S. Paunonen[1], E. Pääkkönen[1], T. Pöhler[1], T. Turpeinen[1], A. Miettinen[2], T. Mäkinen[3], J. Koivisto[3] and M. J. Alava[3]

[1] VTT Technical Research Centre of Finland Ltd, P. O. Box 1000, FI-02044 VTT, Espoo, Finland
[2] Department of Physics, University of Jyvaskyla, P.O. Box 35, FI-40014 Jyvaskyla, Finland
[3] Department of Applied Physics, Aalto University, P. O. Box 11100, 00076 Aalto, Espoo, Finland

ABSTRACT

We discuss a new mean-field theory to describe the compression behaviour of thick low-density fibre networks. The theory is based on the idea that in very large systems, the statistics of free segment lengths causes the stress-deformation behaviour to be quantitatively predictable. The theoretical ideas are supported by several different experimental characterisations. Firstly, we have carried out single-fibre buckling tests using hemp fibres, which indicate a maximum level of axial stress before deformation localization, after which the load-carrying ability of a fibre decays. Secondly, the stress-compression behaviour of over 130 different foam-formed lightweight fibre materials were measured. For kraft pulps with low fines content, the average stress compression behaviour closely follows the theoretical prediction as described in terms of a universal *s*-function. Moreover, the acoustic emission can be described by the same function until collective phenomena cause deviations from the predicted behaviour. Similar deviations at smaller compressive strains are seen with

furnishes with high fines content or added nanocelluloses together with samples with large voids. The localized buckling deformations lead to rapid stress re-distributions and subsequent fibre displacements in a fibre network as shown with in-situ CCD imaging.

INTRODUCTION

In search for sustainable insulation [1–2], filtering [3–4], packaging [5–6] and construction [7] materials, there is an increasing interest in low-density three-dimensional (3D) fibre networks [8–9]. Materials with a varied density and microporous structure can be produced with foam forming technology [10–11]. The obtained material characteristics lie between those of paper, with well-bonded fibres, and of soft non-wovens (e.g. wool), characterized by a non-planar fibre orientation and long free fibre segments. Despite similar, close to exponential distribution of the segment lengths in all these cases [12], the deformation behaviour of individual segments and the whole material can differ greatly for the above materials.

At a material density below 100 kg/m^3, the free segment lengths between neighbouring inter-fibre joints can get quite long, with only a few contacts per 1–2 mm-long natural fibre. This causes the deformations to be non-affine so that local behaviour can deviate a lot from the average strain [13]. Moreover, new deformation modes may appear with heterogeneous natural fibres. Smooth bending appearing in model simulations [13–14] of the idealized fibre systems can give a wrong picture of the real deformation behaviour.

Besides the measurement of average stress during sample compression, we have studied the deformations with several experimental techniques, including single-fibre buckling tests, in-situ high-speed CCD imaging [15], x-ray tomography, and acoustic emission analysis [16]. This has led to a new theory on the stress behaviour for varied strain based on the inelastic buckling of free segments in a bonded fibre network. The quantitative predictions have been verified using a broad range of lightweight materials with varied raw materials, density and forming conditions.

MATERIALS AND METHODS

Foam Forming of Lightweight Samples

The main raw materials used for material preparation were bleached softwood kraft pulps (BSKP, Metsä Fibre Oy, Äänekoski Bioproduct Mill, Finland) and

spruce chemi-thermo mechanical pulps (CTMP, Rottneros AB, Rottneros Mill, Sweden) of different refining levels [15]. In some of the samples, Finnish hemp bast fibres (Cannabis sativa, HempRefine Oy) were used as an additional larger fibre component [17]. Moreover, different nanocellulose fractions such as cellulose microfibrils (CMF), and TEMPO-oxidized cellulose nanofibrils (TCNF) were included as smaller lignocellulosic material components [17].

The main steps of the material production are illustrated in Figure 1. The chosen fibres were mixed with water and surfactants so that a desired air content and bubble size of the wet fibre foam could achieved. This foam was then poured into a foam forming mould, where the structure drained for 20–40 minutes. The remaining self-standing thick fibre sheet was dried in an oven. After drying, a sample was re-moistened to roughly 50% solids content and pressed to a target thickness of 15–20 mm. The other details of the sample preparation can be found in ref. [15].

The density of the material can be controlled with air content and stability of the foam together with the fibre type and dimensions. The foam properties are determined by the mixing speed and geometry and by the used foaming agents. This study included several foaming agents of different types: anionic sodium dodecyl sulphate (SDS), non-ionic polyethylene glycol sorbitan monolaurate (Tween 20), mixtures of SDS and Tween 20, non-ionic polyvinyl alcohol (PVA 6-88), non-ionic alkyl polyglucoside (APG), and a mixture of non-ionic and cationic surfactants (Berol ENV226 Plus).

We prepared around 130 different materials by varying the foam forming conditions in a wide range. The consistency of the suspension was varied in the range of 1% to 8%, while the air content of wet foam was 39–79%, and the final material densities varied in the range of 20–120 kg/m^3 (the most frequent levels were 40 kg/m^3 and 80 kg/m^3).

The characterization of these materials included measurements of the grammage, thickness, and density together with x-ray tomography on some of the
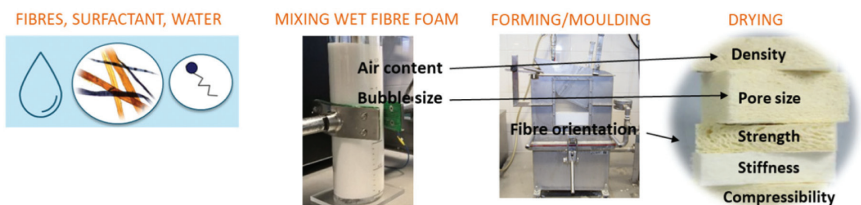

Figure 1. Foam forming procedure to obtain lightweight fibre materials with varied structural and mechanical properties.

samples. For mechanical testing, the large sheet samples of size 21 cm × 35 cm were cut to smaller parallel samples with the area of 5 cm × 5 cm.

Mechanical Testing and Related Characterization

Most of the compression measurements were carried out with a Lloyd LR10K universal tester (Lloyd Instruments Ltd, Bognor Regis, West Sussex, UK). The test speed was 10%/min for the first compression up to 10% strain and 100%/min for the subsequent cycles. Cyclic testing allowed us to follow not only the resilience but also the acoustic emission [16] of the samples during de-loading. Moreover, the deformation behaviour was analysed for some samples with in-situ high-speed CCD imaging using image correlation techniques [15] and x-ray tomography. Five parallel measurements were taken for each trial point.

The acoustic emission measurements were based on smaller samples ($19 \times 20 \times 20$ mm^3) than the rest of the compression measurements [16]. In this case, the load-displacement behaviour was measured with an Instron E1000 tensile testing machine, and an AE sensor was attached to a thin plastic plate covering the compressed sample. The amplified acoustic signal during measurement was digitized for further analysis. The details of the experimental setup can be found in ref. [16]. The averaged results were based on 10 parallel measurements.

Single-fibre Buckling Tests

We studied the buckling of single hemp bast fibres using a measurement setup designed specifically for single-fibre mechanical testing [18]. The chemical composition of hemp fibres is similar to wood fibres, but their larger size helps in fibre handling, visual observation and force measurement. Hemp fibres contain 81% cellulose, 11% hemicellulose, and 5% lignin [17]. After treating the fibres with a Kvarn BAHS-30 hammer mill (Kamas Industri AB), they went through a soda cooking process [17], which led to flat fibre bundles with a thickness of c.a. 50 μm and a width of c.a. 120 μm. For large applied strains, the compression test often led to a splitting of a bundle into smaller ones. 28 parallel tests were carried out with varied free span lengths in the range of 1100–2100 μm and with different fibre shapes and dimensions.

BUCKLING OF SINGLE FIBRES

An example of the buckling measurement of a single hemp fibre is shown in Figure 2. One end of the fibre is fixed while the other end collides with a moving wall that gradually increases the (negative) apparent strain. No sliding of the free

fibre end was observed during testing. Under the induced compressive stress, the precise way a fibre bends or buckles depends on its tilt and curliness. This affects the recorded force-strain curve. Despite a large scatter in the observed behaviour in the parallel tests, the following features were generally repeated:

- The compressive stiffness of the fibres was very low in all measurements (Figure 2b).
- All measured (compressive) forces achieved a maximum level at a strain that generally depended on the fibre slenderness. This strain was relatively small (2–5%) for the slenderest fibres, whereas for short spans and thick fibres the maximum force was achieved at strains exceeding 10%. The strain beyond which the force either dropped immediately (Figure 2b) or remained on a plateau was large enough so that the deformation could be expected to be inelastic.
- The main deformation localized to a certain axial region of the bent fibre near the maximal force. For some very straight fibres, the localization could be preceded by a buckling deformation into a bent shape. However, the maximal force was achieved very soon after that.
- Recovery from localized buckling was poor. In a repeated buckling test for the same fibre, the maximum force was clearly lower for the 2nd test.

As shown in Figure 2c, the maximal compressive force achieved before localization of the deformation (Figure 2b) correlated with the slenderness ratio, $a/\sqrt{I/A}$. Here a is the span length, A is the cross-sectional area of a fibre, and I is the minimum area moment of the inertia of the cross section [mm^4],

$$I = wt^3/12, \qquad (1)$$

as expressed in terms of the average width w and thickness t of a hemp fibre with a roughly rectangular cross-section. A similar power-law correlation as for the force was found also for the apparent buckling strain, determined from the reduced horizontal span at the turning point of the force-strain curve (Figure 2d). In many cases, this corresponded to the localization of the deformation whereas the actual buckling of a fibre had already taken place a bit earlier.

There was a rather large variation in the cross-sectional area and compressive modulus E in the measurements. Still, the measured maximal compression force followed Euler's equation

$$F = \mu \frac{\pi^2 EI}{a^\alpha} \qquad (2)$$

The correlation between the measurements and Eq. (2) was quite good ($R^2 = 0.980$ – 0.984) in a wide range, 1.0–2.6, of values of the power α. In other words, the force F was dominated by I rather than the span a. The situation might be different in a bonded fibre network where both primary and a-dependent secondary moments appear. In Figure 3 we show the correlation for $\alpha = 2$, a value compatible with dimensional analysis.

Originally, the factor μ in Eq. (2) describes the effects of boundary conditions at the ends, varying typically in the range of 1–4. However, in our measurements for hemp fibres, we obtained a much larger value of $\mu \approx 18$ (Figure 3). It is possible
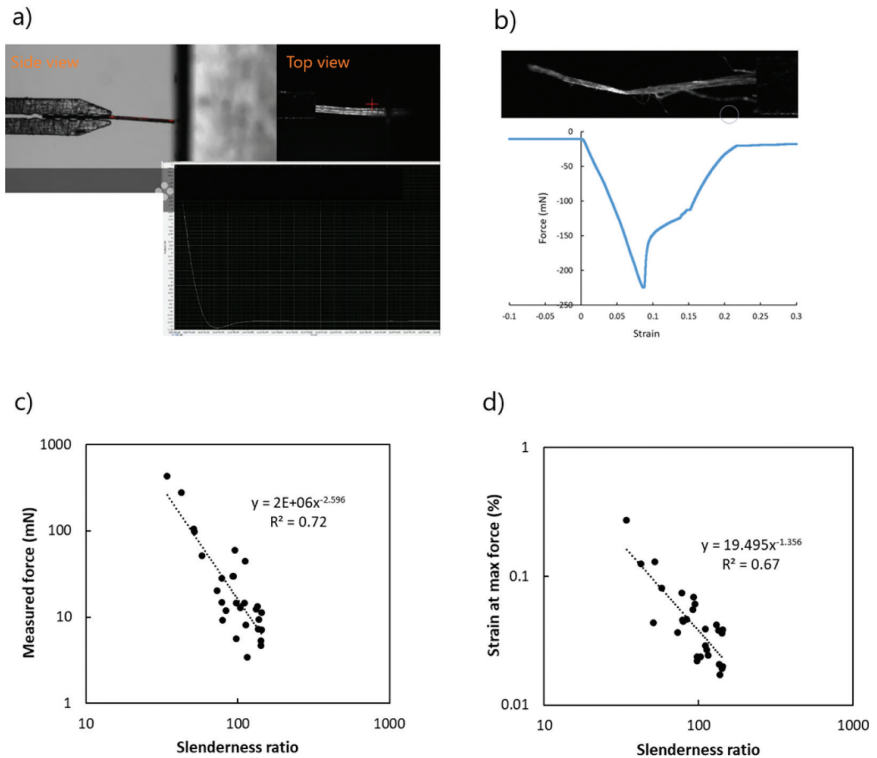

Figure 2. Buckling measurements for single hemp fibres: (a) Experimental setup showing both side and top images of a tested fibre. (b) Force-strain curve of a single measurement. The absolute compressive force drops after localization of the buckling in the fibre. (c, d) Measured maximal compression force and corresponding apparent strain as a function of the slenderness ratio. The measured data contains varied span lengths in the range of 1–2 mm.
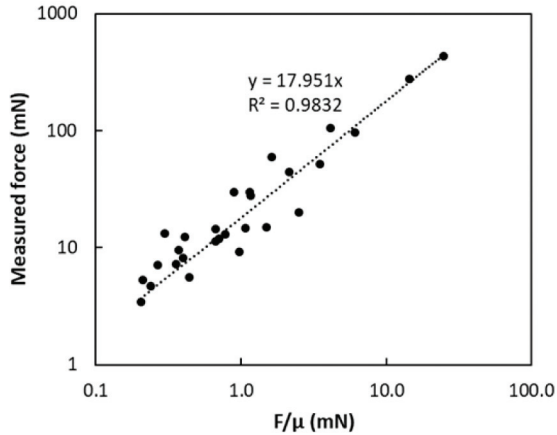
Figure 3. Measured force of hemp buckling measurements plotted against Euler's equation for $\alpha = 2$.

that this high value somehow compensates for the low compression modulus, 0.17 ± 0.07 GPa, obtained in the buckling measurements. Even though one generally expects a smaller value for compression than for a tensile test, the average compression modulus was surprisingly small compared to the average tensile modulus of 30–60 GPa measured earlier for hemp fibres [19]. The compressed fibres may experience internal viscoelastic and plastic deformations already before buckling, which could be seen in the determined modulus value.

NEW THEORY ON THE COMPRESSION BEHAVIOUR

We propose that in low-density fibrous materials, the increasing axial stress in fibres during compression, as predicted by Subramanian and Picu [13], can be released by a buckling of the corresponding heterogeneous fibre segment, causing a possible simultaneous displacement of neighbouring fibres and rapid changes in the overall stress field. In a random fibre network, the distribution of fibre segment lengths is exponential:

$$p(a) = \frac{1}{a_0} \exp\left(-\frac{a}{a_0}\right) \tag{3}$$

As illustrated in Figure 4, the longest segments get the least support from the neighbouring fibres and therefore these segments are expected to buckle first. We
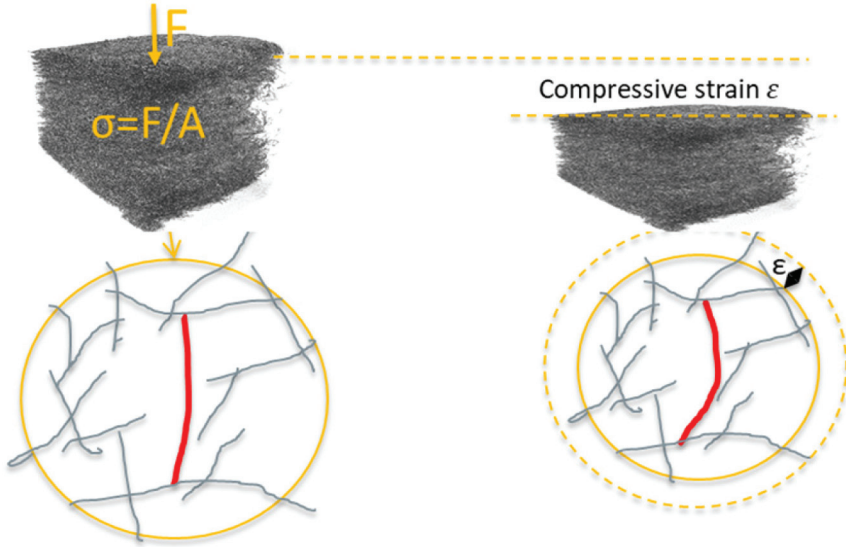
Figure 4. A long free fibre segment (shown in red) buckles inside a low-density fibre network under the stress induced by the average compressive strain ϵ. For initially curly and bent segments, the buckling would correspond to localization of the main plastic deformation as described in the single-fibre buckling tests.

describe this tendency with a function $s(\varepsilon)$ by assuming that at strain ϵ, segments longer than $a_0 s(\epsilon)$ have buckled, where a_0 is the mean segment length [15]. The relative number of buckled segments at strain ϵ becomes

$$\int_{a_0 s(\varepsilon)}^{\infty} p(a)da = e^{-s(\epsilon)} \tag{4}$$

This equation could also be taken as the definition of function $s(\varepsilon)$ for a more general distribution of segment buckling, as illustrated in Figure 5a. In this way, the statistical variation in the deformation behaviour can be taken into account. The mean length of the remaining non-buckled fibre segments is

$$\int_{0}^{a_0 s(\varepsilon)} ap(a)da = a_0 \left[1 - \left[s(\epsilon) + 1 \right] e^{-s(\epsilon)} \right] \tag{5}$$

Because a buckled segment deforms easily within the porous structure without extra force (compared to the corresponding maximal force), the non-buckled segments span the deformed network whose thickness has been reduced by the factor ϵ. Thus, it is natural to assume that
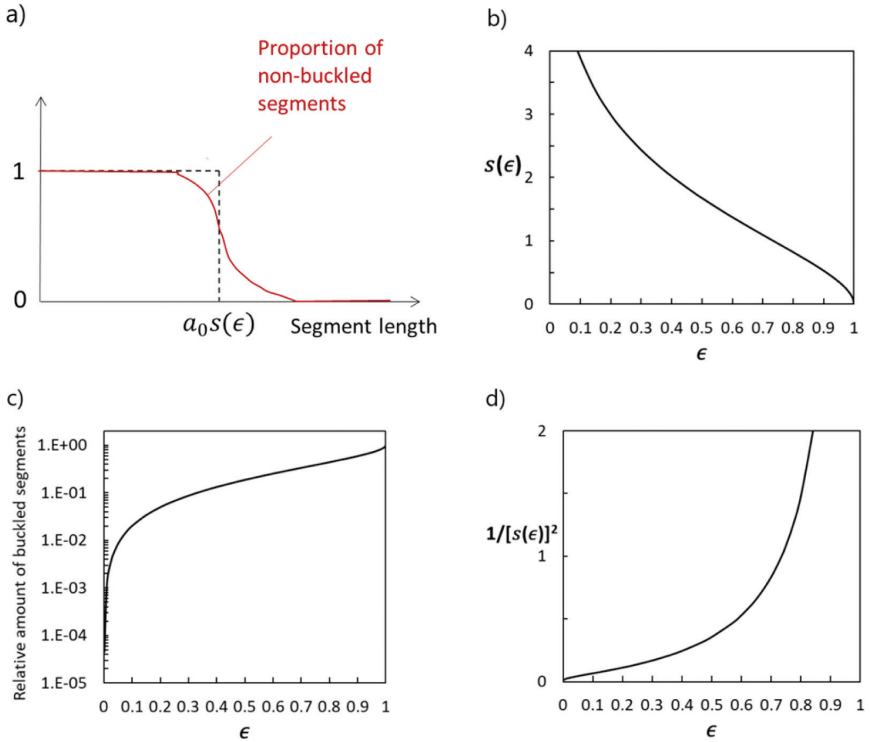
Figure 5. (a) The proportion of non-buckled segments for varied segment length is described by a step function. (b) The universal function $s(\epsilon)$. (c) The relative number of buckled segments as a function of strain ϵ as described by the function $e^{-s(\epsilon)}$. (d) Function $1/s(\epsilon)^2$ that describes the relative behaviour of the compression stress.

$$[s(\epsilon) + 1]e^{-s(\epsilon)} = \epsilon \qquad (6)$$

from which the function $s(\varepsilon)$ can be solved:

$$s(\epsilon) = -1 - W_{-1}(-\epsilon/e). \qquad (7)$$

Here W_{-1} is the second principal branch of the Lambert W function [16, 20]. Using Eq. (7) or solving s implicitly from Eq. (6) allows us to plot the relative number of buckled segments $e^{-s(\epsilon)}$ as a function of strain ϵ (Figure 5c). This plot suggests that buckling is rare up to about 20% compression, after which their number gradually increases as shorter and shorter segments buckle as indicated by Figure 5b.

If we now assume that the average stress required for buckling at strain ϵ is inversely proportional to the square of the critical segment length $a_0 s(\epsilon)$, as suggested by Figure 3, the mean compressive stress σ is given by

$$\sigma(\epsilon) = \frac{\sigma_0}{[s(\epsilon)]^2} \tag{8}$$

Here the constant σ_0 sets the absolute level of compression stress, while the stress-compression behaviour is described by the same function $s(\epsilon)$ for all low-density random fibre networks with exponentially distributed segment lengths. In other words, the fibre type or bonding properties would affect only the coefficient σ_0. The relative change of stress as a function of the strain can be seen in Figure 5d. Contrary to stress-strain curves of cellular solids [21], there is no intermediate plateau region, and the stress blows up at high strains because of an increasing number of short segments carrying the load rather than because of material densification.

According to this theory, segments with mean length a_0 buckle at rather high average strain of $2e^{-1} \approx 0.736$. On the other hand, the mean segment length can be estimated based on the fibre density ρ_f and material density ρ using a formula developed for an isotropic random network [15, 22],

$$a_0 = \frac{D\rho_f}{2\rho}, \tag{9}$$

where D is the diameter of fibres with circular cross-section. If we assumed that this segment length should exceed e.g. at least two fibre diameters to make a buckling deformation feasible, we would get an estimate of $\rho < \rho_f/4$ for the required material density. For typical wood fibres with lumen $\rho_f \approx 1000$ kg/m³, and thus this buckling theory would become relevant at a material density below 250 kg/m³. This is roughly the level beyond which non-affine deformations have been observed for paper sheets [23].

In the following sections, we provide experimental evidence for this strong prediction based on different types of samples and characterisations. Earlier papers have considered certain universal parameters, derived from Eq. (8) such as the ratio of stresses measured at 50% and 10% compression levels [15],

$$\frac{\sigma(0.5)}{\sigma(0.1)} = \left[\frac{s(0.1)}{s(0.5)}\right]^2 \approx 5.374 \tag{10}$$

or the slope of the stress-strain curve scaled by the stress level [17],

$$\frac{1}{\sigma}\frac{d\sigma(\varepsilon)}{d\varepsilon} = \frac{2[s(\varepsilon)+1]}{\varepsilon[s(\varepsilon)]^2}. \tag{11}$$

The latter slope should have a universal value e.g. at 50% compression,

$$\frac{1}{\sigma}\frac{d\sigma}{d\epsilon}(\epsilon = 0.5) = \frac{4[s(0.5)+1]}{[s(0.5)]^2} \approx 3.804 \tag{12}$$

In the next section, we carry out the validation for the whole stress-strain curve over an extended set of samples.

COMPARISON WITH EXPERIMENTS

Statistical Validation of the Stress-compression Behaviour

We have tested the universal prediction of Eq. (8) for the strain-compression behaviour for a wide range of foam-formed fibre materials. Some of these studies have been reported earlier [15–17]. Typical lightweight fibre samples contain imperfections such as rough surfaces and voids (Figure 6) so that based on just one sample, a perfect agreement with the measured and predicted curves could be found rather seldom. However, the contribution of these imperfections could be expected to be averaged out for a large set of samples. In Figure 7, we make a comparison for the first time between the average stress-compression curve of a very large set of different trial points and the theoretical prediction of Eq. (8).

In Figure 7a, we show the average of 63 kraft-fibre trial points, with different refining levels in pulp preparation, surfactants in foam forming, forming consistencies (1–8%), air contents (44–79%) of the wet foam, and the densities (21–96 kg/m³) of the final material. The compression testing was done cyclically, where the
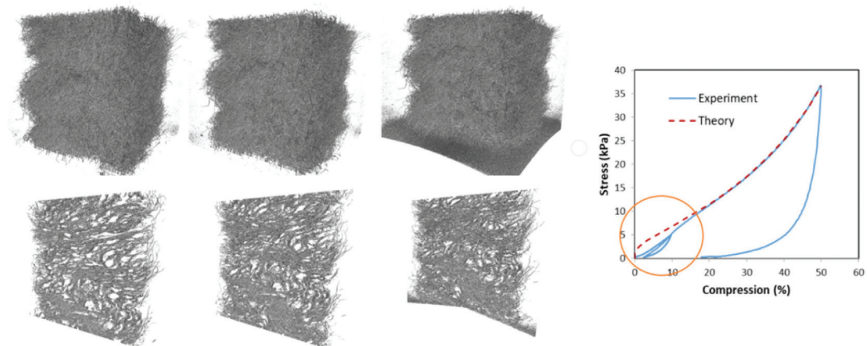

Figure 6. The 3D x-ray tomography images on the left show a kraft-fibre sample (64 kg/m³) with increasing compression. The gradual closing of the largest voids can be seen in the thinner slices of these structures shown on the bottom. Closing the voids affects the initial stress-compression curve under 15% strain as shown in the right figure.
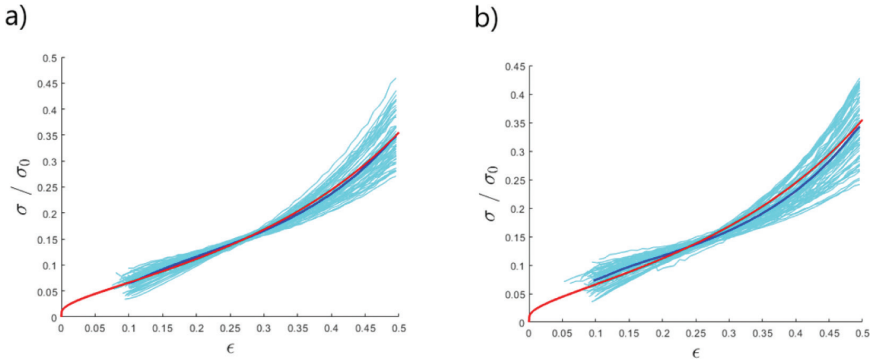
a)

b)

Figure 7. Scaled stress-strain behaviour of different trials points with (a) kraft and (b) CTMP fibres (light blue curves are averages of 5 parallel measurements for different trial points). The dark blue curve shows the average over all trial points, which is compared to the theoretical prediction of Eq. (8) (red curve). CTMP contains a large quantity of fines, which affects the average behaviour.

first compression extended to 10% strain and the second one to 50% strain. For each trial point, an average curve of 5 parallel measurements was determined in the range of 10–50% strain (i.e. based on the 2nd compression). We fitted σ_0 for each trial point so that the separation of the average curve was smallest (using the least square method) to the theoretical curve. Each light blue curve in Figure 7a is such an average. The dark blue curve is the average of all trial points that matches with the theoretical prediction (red curve) very well. The low (c.a. 10 w%) quantity of fines in kraft pulps makes the assumption of the statistics of free-span lengths reasonable, which is an important factor behind the observed agreement. The total area of tested material to produce Figure 7a was about 0.8 m^2.

In an earlier study [17] with added fines and nanocelluloses (Figure 8), we found that the stiffening of the initial part of the stress-compression curve was probably caused by the multi-scale network structure. Similar effects can be seen in Figure 7b when plotting the average stress-compression curve of 68 CTMP trial points. These samples contain a lot more fines (c.a. 30 w%) than the kraft samples. With CTMP, the overall scatter of the curves for varied trial points is larger than in Figure 7a for the kraft pulps. In Figure 7b, also a slightly larger density range of 21–124 kg/m^3 was included than in Figure 7a.

Besides the stress-strain behaviour, further support for the above theoretical ideas comes from studying the average stress at a chosen compression level for a varied material density and constant fibre type. According to Eq. (9), the mean
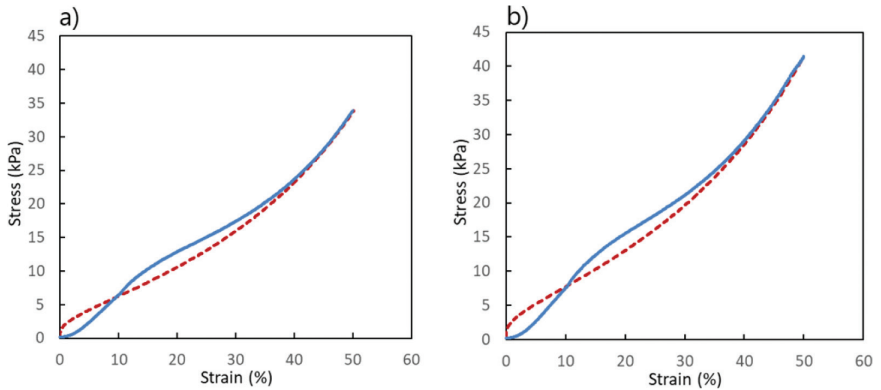
Figure 8. Comparison of the measured compression behaviour (solid curve) to the theoretical prediction of Eq. (8) (dashed curve) for structures made with unrefined kraft pulp (80%) and hemp fibres (20%) with added a) cellulose microfibrils and starch, and b) TEMPO oxidized cellulose nanofibrils and starch. Despite the initial deviations, the slope defined by Eq. (12) for 50% strain is close to the theoretical value of 3.804 in both cases. For figure a, the measured slope is 3.86 ± 0.18, and for figure b the value is 3.88 ± 0.15. Reprinted from ref. [17] under the terms of the CC BT 4.0 license.

segment length is inversely proportional to the material density. Thus, the absolute stress level should be proportional to the square of this density based on Eq. (2). Such an approximate square dependence is indeed observed experimentally for several fibre types [6, 15], provided the density is high enough to prevent consolidation of fibres into separate layers [9]. In particular, the experimental behaviour of bonded fibre networks usually differs from the cubic dependence, which has been suggested earlier by assuming fibre bending to be the principal deformation mode [24].

Predicting Acoustic Emission

Cyclic compression tests indicate that the measured acoustic emission during compression cannot be caused by smooth fibre bending. Fibres bend also during unloading but this does not cause a measurable acoustic emission. A significant acoustic emission is recorded only when the compression exceeds previous levels [16]. Possible other acoustic emission sources could be due to aspects such as the opening of fibre joints and plastic yielding of buckling fibres.

Interestingly, the development of acoustic energy emission during compression can be directly linked to the relative amount of segment buckling $e^{-s(\epsilon)}$ (Figure 9).

Our measurements for kraft samples with a density of 64 kg/m^3 [16] show that the number of acoustic events for small and moderate strains is given by the function $e^{-\alpha s(\epsilon)}$ with α in the range 2.8–3.0. We would like to emphasize that in this comparison α is the only fitting parameter, because there is only one way to normalize the measured acoustic emission so that it equals $e^{-\alpha s(\epsilon)}$ at strain ϵ where the measurement is stopped. Thus, the fact that the measured data follows $e^{-\alpha s(\epsilon)}$ for low ϵ-values in Figure 9a is highly nontrivial as the absolute scale is set by the above normalization.

At strains exceeding 0.5 (i.e. 50%), collective phenomena with bursts of several simultaneous buckling can lead to deviations from this simple behaviour [16]. This affects the stress-compression behaviour as well so that the measured stress is higher than the predicted one for large strains.

In-situ CCD Imaging of Network Deformations

Besides visualizing single fibre buckling and macroscopic material deformations, it is interesting to try to capture rapid network deformations during compression. We used high-speed CCD imaging to follow dynamic changes in the open structure through a side of a compressed sample [15] (Figure 10). The network deformations turned out to be very heterogeneous, with alternating still and rapidly changing material regions. Moreover, different fibres could respond very differently even in a same small region as shown in Figure 10. The correlation analysis between subsequent video frames revealed sudden local fibre displacements during a very short time step. This suggested rapid stress re-distributions inside the fibre network, which is in agreement with the postulated fibre buckling as an important deformation mode.
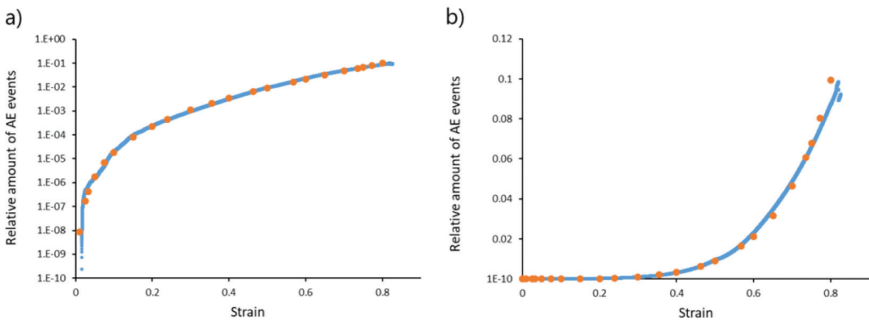

Figure 9. Relative number of acoustic events during compression of a kraft sample (blue curve) compared to the function $e^{-\alpha s(\epsilon)}$ with $\alpha = 2.8$ (orange dots) in both a) logarithmic and b) linear scales [16].
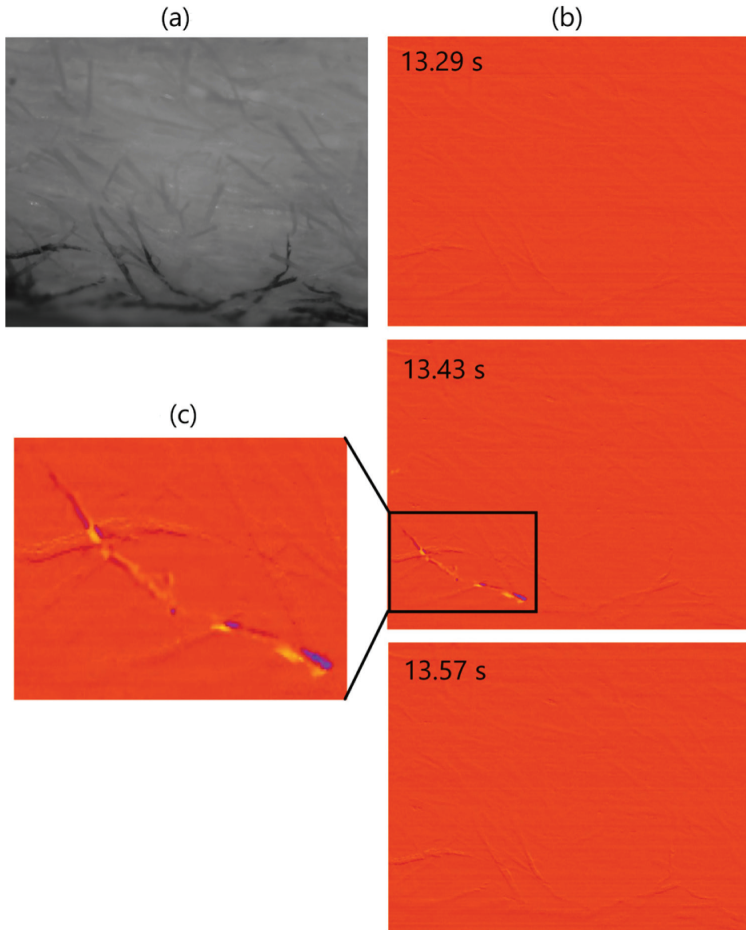
Figure 10. The local response of a CTMP sample (density 71.9 kg/m³) during compression (speed 100%/min) is heterogeneous as revealed by high-speed CCD imaging: a) The fibre network of the imaged area (6.7 mm × 5.4 mm), where a part of the fibres have been coloured black. b) Correlation maps [25] for three subsequent image frames. Orange colour indicates a high correlation between the corresponding frame and the preceding one. Thus, at times 13.29 s and 13.57 s, for which no other colours are visible, the local network deforms only very little between subsequent frames. However, at the intermediate time 13.43 s (strain 17.8%), a rapid fibre displacement inside the square region leads to a lower correlation as indicated by the colour change. c) The blowup of the square region shows the displacement and the change in the curvature of a fibre (yellow=old location, blue=new location).

CONCLUSIONS

Novel forming processes such as foam forming enable the production of light-weight fibre materials whose density is clearly below that of typical paper. In applications, the compression behaviour is often the most important mechanical property because of the open porous structure of these thick materials. During compression, individual fibres have a large amount of freedom to respond to changing stress field as their relative bonded area is small. This can lead to heterogeneous, rapidly changing strain field on a microscale and to new deformation modes for the fibres. We propose that gradually increasing the axial stress in fibres during material compression can lead to them buckling where a significant part of the load-carrying ability is lost, and that the buckling probability of a segment depends on its span length. This has led to simple equations describing the stress development, whose ability to predict the measured stress with reasonable accuracy has been verified using a very large set of low-density fibre materials with different densities and fibre types. Moreover, the derived function that describes the relative amount of segment buckling seems to describe the acoustic energy emission also for small and moderate strains. A curious feature is that for relative stress changes during compression, the statistics of the structure become more important than the mechanical fibre properties. Thus, we expect our theory to have applicability also to other types of bonded fibrous networks.

ACKNOWLEDGEMENTS

REFERENCES

[1] Madani, A., Zeinoddini, S., Varahmi, S., Turnbull, H., Phillion, A. B., Olson, J. A. and Martinez, D. M. (2014) Ultra-Lightweight Paper Foams: Processing and Properties. *Cellulose* 21 (3): 2023–2031. https://doi.org/10.1007/s10570-014-0197-3

[2] Pöhler, T., Jetsu, P., Fougerón, A. and Barraud, V. (2017) Use of papermaking pulps in foam-formed thermal insulation materials. *Nord. Pulp. Pap. Res. J.* 32: 367–374. https://doi.org/10.3183/npprj-2017-32-03-p367-374

[3] Jahangiri, P., Korehei, R., Zeinoddini, S. S., Madani, A., Sharma, Y., Phillion, A., Martinez, D. M. and Olson, J. A. (2014) On filtration and heat insulation properties of foam formed cellulose based materials. *Nord. Pulp. Pap. Res. J.* 29: 584–591. https://doi.org/10.3183/NPPRJ-2014-29-04-p584-591

[4] Heydarifard, S., Nazhad, M. M., Xiao, H., Shipin, O. and Olson, J. (2016) Water-resistant cellulosic filter for aerosol entrapment and water purification, Part I: Production of water-resistant cellulosic filter. *Environ. Technol.* 37 (13): 1716–1722. https://doi.org/10.1080/09593330.2015.1130174

[5] Bunker, D., Cecchini, J., Hietaniemi, M., Virtanen, M., Torvinen, K., Asikainen, J. and Salminen, K. Foam forming technology folding box board focused developments. In *Paper Conference and Trade Show (PaperCon 2017);* TAPPI: Minneapolis, 2017, p 1802.

[6] Liao, J., Luan, P., Zhang, Y., Chen, L., Huang, L., Mo, L., Li, J. and Xiong, Q. (2022) A lightweight, biodegradable, and recyclable cellulose-based bio-foam with good mechanical strength and water stability. *J. Environ. Chem. Eng.* 10: 107788. https://doi.org/10.1016/j.jece.2022.107788

[7] Pöhler, T., Jetsu, P. and Isomoisio, H. (2016) Benchmarking new wood fibre–based sound absorbing material made with a foam-forming technique. *Build. Acoust.* 23: 131–143. https://doi.org/10.1177/1351010X16661564

[8] Alimadadi, M. and Uesaka, T. (2016) 3D-oriented fibre networks made by foam forming. *Cellulose* 23: 661–671. https://doi.org/10.1007/s10570-015-0811-z

[9] Burke, S. R., Möbius, M. E., Hjelt, T., Ketoja, J. A. and Hutzler, S. (2021) Analysis of the foam-forming of non-woven lightweight fibrous materials using X-ray tomography. *SN Appl. Sci* 3: 192. https://doi.org/10.1007/s42452-021-04172-9

[10] Radvan, B. and Gatward, A. P. J. (1972) The formation of wet-laid webs by a foaming process. *Tappi J.* 55: 748–751.

[11] Hjelt, T., Ketoja, J. A., Kiiskinen, H., Koponen, A. I. and Pääkkönen, E. (2021) Foam forming of fibre products: a review, *J. Dispersion Sci. Techn.* https://doi.org/10.1080/01932691.2020.1869035

[12] Sampson, W. W. (2008) Unified theory for structural statistics of flocculated and random fibre networks. *J. Pulp Pap. Sci.* 34: 91–98.

[13] Subramanian, G. and Picu, C. R. (2011) Mechanics of three-dimensional, nonbonded random fibre networks. *Phys. Rev.* E 83: 056120. https://doi.org/10.1103/PhysRevE.83.056120

[14] Alimadadi, M., Lindström, S.B. and Kulachenko, A. (2018) Role of microstructures in the compression response of three-dimensional foam-formed wood fiber networks. *Soft Matter* 14: 8945–8955. https://doi.org/10.1039/C7SM02561K

[15] Ketoja, J. A., Paunonen, S., Jetsu, P. and Pääkkönen, E. (2019) Compression strength mechanisms of low-density fibrous materials. *Materials* 12: 384. https://doi.org/10.3390/ma12030384

[16] Mäkinen, T., Koivisto, J., Pääkkönen, E., Ketoja, J. A. and Alava, M. J. (2020) Crossover from mean-field compression to collective phenomena in low-density foam-formed fibre material. *Soft Matter* 16: 6819–6825. https://doi.org/10.1039/d0sm00286k

[17] Pöhler, T., Ketoja, J. A., Lappalainen, T., Luukkainen, V.-M., Nurminen, I., Lahtinen, P. and Torvinen, K. (2020) On the strength improvement of lightweight fibre networks by polymers, fibrils and fines. *Cellulose* 27: 6961–6976. https://doi.org/10.1007/s10570-020-03263-x

[18] Laurikainen, P., Kakkonen, M., von Essen, M., Tanhuanpää, O., Kallio, P. and Sarlin, E. (2020) Identification and compensation of error sources in the microbond test utilising a reliable high-throughput device. *Composites Part A: Applied Science and Manufacturing* 137: 105988. https://doi.org/10.1016/j.compositesa.2020.105988

[19] Shahzad, A. (2012) Hemp fiber and its composites – a review. *J. Compos. Mater.* 46(8): 973–986. https://doi.org/10.1177/0021998311413623

[20] Corless, R. M., Gonnet, G. H., Hare, D. E. G., Jeffrey, D. J. and Knuth, D. E. (1996) On the Lambert W Function. *Advances in Computational Mathematics* 5: 329–359. https://cs.uwaterloo.ca/research/tr/1993/03/W.pdf

[21] Gibson, L. J. and Ashby, M. F. (1997) *Cellular Solids: Structure and Properties*. 2nd edn, Cambridge University Press.

[22] Komori, T. and Makishima, K. (1977) Numbers of fiber-to-fiber contacts in general fiber assemblies. *Text. Res. J.* 47: 13–17. https://doi.org/10.1177/004051757704700104

[23] Picu, R. C. (2011) Mechanics of random fiber networks—a review. *Soft Matter* 7: 6768–6785. https://doi.org/10.1039/c1sm05022b

[24] van Wyk, C. M. (1946) Note on the compressibility of wool. *J. Text. Inst. Trans.* 37: T285–T292. https://doi.org/10.1080/19447024608659279

[25] Chinga, G. and Syverud, K. (2007) Quantification of paper mass distributions within local picking areas. *Nord. Pulp Pap. Res. J.* 22: 441–446. https://doi.org/10.3183/NPPRJ-2007-22-04-p441-446

MEAN-FIELD APPROACH TO COMPRESSION OF THICK POROUS FIBRE NETWORKS

J. A. Ketoja[1]*, S. Paunonen*[1]*, E. Pääkkönen*[1]*, T. Pöhler*[1]*,*
T. Turpeinen[1]*, A. Miettinen*[2]*, T. Mäkinen*[3]*, J. Koivisto*[3]
and M. J. Alava[3]

[1] VTT Technical Research Centre of Finland Ltd, P. O. Box 1000, FI-02044
VTT, Espoo, Finland
[2] Department of Physics, University of Jyvaskyla, P.O. Box 35, FI-40014
Jyvaskyla, Finland
[3] Department of Applied Physics, Aalto University, P. O. Box 11100,
00076 Aalto, Espoo, Finland

Daniel Söderberg   KTH Royal Institute of Technology

I am very interested in the mechanics and if you would start instead by assuming that you are looking at bending and would build everything from that, how different would it be when it comes to your results? Would that be an alternative way of doing the modelling?

Jukka Ketoja

Well, people have done it a lot historically. Van Wyk started that after the second world war. He looked at the fibre bending model for wool and compared that with wool data. In this case, the fibres slide, they are not bonded. There is no reason for a fibre buckling in this kind of material. Later, other people have looked more carefully at this kind of phenomena using various models. The main difference to my mind is that the density dependence goes like the power of three instead of two, and of course we have guys like Artem Kulachenko and others who can simulate it. So we have all kinds of techniques to look at that. But the essence here

Discussion

is that a buckling gives you the stress tensor, while bending does not give it in a similar fashion.

Artem Kulachenko   Royal Institute of Technology (KTH)

Thank you for the fascinating presentation. I have a follow-up on the bending story. What you could see even in the tomography data, fibre bending dominates in the overall deformation. You can also see that when you do the tensile testing and compression testing, they both show more or less the same results, at least to a certain strain. You also recognised that buckling happens at a later stage of the process. But then, if I understood correctly, you said that the effect of the initial density is not so evident. You also said that buckling happens with the shortest segments in the densified regime with many overstressed segments appearing. Should the initial density play a role then?

Jukka Ketoja

Yes, in principle it could. However, when you are below 100 kg/m^3 density, the porosity is really very high to start with, for example 99%, and then you can compress the material quite far so that you still have very high porosity. That is why there is a lot of room for fibres to deform and buckle without colliding. The equations would not care about how many fibres buckled, they would look more or less the same. There is no statement about that. But intuitively it is clear that for shorter segments the buckling is more probable because both the cellulose fibres and the bonds are quite stiff. So, when you shorten the segment, it is harder and harder to just easily start bending, and for that reason some of the samples, e.g. those containing nano-cellulose, have to be compressed pretty far in order to activate those segments which are short enough so that it is difficult for them to bend. Of course, the longer segments bend nicely and they have more freedom to do that.

Artem Kulachenko

And they also have an initial curvature which is promoting bending. Regarding the fibre compression experiment that you demonstrated: we have a similar device, and we could not create conditions for such nice buckling. We always see bending because you have to grasp the fibre, it has to be straight and also you need to point into the surface very carefully. We always see bending and we could not succeed in doing this.

Jukka Ketoja

Did you see localisation of deformation after a fibre bent? I think that should at some point occur because when you exceed a few percent strain, you will go to the inelastic plastic region for the fibre wall, and it will respond with localised buckling.

Warren Batchelor   Monash University

I'm curious, are your foam form structures isotropic in all their directions and how do you account for any anisotropy in your models?

Jukka Ketoja

Well, we do not do it in any way at the moment, and the structures are not isotropic. In foam forming, especially when you decrease the density, you easily get a partly layered structure. If you turn such a sample on its side, the layers can buckle when you compress it. You will have a different response which looks more like that of cellular solids. So, this theory does not explain everything.

Alexander Bismarck   University of Vienna

Your model . . . what would it tell me about how to make better foams without using polymers or fines and micro/nanocellulose to support bonding between the fibres? I am interested in foams and want to produce better fibre foams, tell me please which fibres I ought to use?

Jukka Ketoja

I don't know if the theory answers to that question. It rather says that if you have fibres to make cushioning materials, different fibre materials even when you change the fibre type respond pretty similarly. This response will be pretty soft and maybe good for some applications. If you want to have stiffer response like for expanded polystyrene (EPS), then you have to add some hierarchical structure in the material. With just a simple random fibre network you do not get it.

Alexander Bismarck

That means you have to support your fibres.

Discussion

Jukka Ketoja

Yes, if you need that response. I do not know if the EPS response is the best for everything. Maybe for a washing machine it's a good response, if you drop it. But maybe for glass a softer response would be better.

Anton Hagman   RISE Research Institutes of Sweden

I have two short questions. How dense is 'not so dense' in a not so dense network? What is the limit for the density? Do you have any feeling about that?

Jukka Ketoja

As I mentioned, in order to have buckling at all, you have to go down to 250 kg/m^3 or below, but how well the theory would apply I am not sure. The highest density where we show it to work very well is around 130 kg/m^3. This kind of intermediate density range is a bit unexplored region for fibre materials. So there is work to do.

Anton Hagman

And one other short question because they had this kind of cubic samples, did you test very thin samples to compress or thinner samples?

Jukka Ketoja

Yes, the thickness was 1.5 cm for the thinnest, and it works pretty well, as you have lots of fibres.

Ulrich Hirn   Graz University of Technology

In classical beam theory for buckling you have a continuous beam with constant bending stiffness. When we look at the failing process of the fibres, in these fibres you have a curled structure which has local variations in bending stiffness. So to me, maybe, this is a continuum between bending failure and true buckling. So, I am wondering if buckling is exactly the right term because we have this inhomogeneity in bending stiffness and very little tensile load on the failures, which is also characteristic for buckling. So, to me, it looks a little bit like local failure under bending load.

Jukka Ketoja

I both agree and disagree. I fully agree with the first point you said that there are local variations in fibre bending stiffness. I am also wondering whether the word "buckling" is the right one, but I am a Finn. I took the word which indicates a kind of sudden bifurcation in the deformation behaviour because I am pretty sure some kind of buckling takes places within the fibre wall. Something quite sudden happens as we see in the tomography with red lights (indicating that local deformation deviates from an affine transformation) coming and going away. It's this sudden bifurcation which we should do research on.

As to the second point, I believe there will be quite high axial stresses because the short segments have strong boundary conditions coming from the bonds, and when you deform that part of the network, they experience axial stresses for sure.

Ulrich Hirn

Yes, that is right. The shorter segments are under tensile stress for sure.

Jukka Ketoja

Yes. So, it's not black and white of course, and I do not want to give that message. We have all the beauty of variety in the behaviour.

Daniel Söderberg

Looking at the paper, the relation between stress and strain you have is proportional to the buckling length to the power of 2, which I guess is the same relationship you would get in a beam with a point load. So, is it actually possible to separate these two phenomena since they have the same stress-strain coupling relation?

Jukka Ketoja

Yes, I think it is, and that's the area where we need to do more research. As you saw the characterisation was mainly done for large volumes with for example the acoustic method. But maybe that is why I said the second slide was the most important. I think we have underestimated the stiffness of the fibre as to its deformation behaviour; that is just my opinion.